
Sonic4D: Spatial Audio Generation for Immersive 4D Scene Exploration

Siyi Xie* Hanxin Zhu* Tianyu He Xin Li† Zhibo Chen†

University of Science and Technology of China

{ustc2020xxy, hanxinzhu}@mail.ustc.edu.cn, {xin.li, chenzhibo}@ustc.edu.cn

Abstract

Recent advancements in 4D generation have demonstrated its remarkable capability in synthesizing photorealistic renderings of dynamic 3D scenes. However, despite achieving impressive visual performance, almost all existing methods overlook the generation of spatial audio aligned with the corresponding 4D scenes, posing a significant limitation to truly immersive audiovisual experiences. To mitigate this issue, we propose **Sonic4D**, a novel framework that enables spatial audio generation for immersive exploration of 4D scenes. Specifically, our method is composed of three stages: 1) To capture both the dynamic visual content and raw auditory information from a monocular video, we first employ pre-trained expert models to generate the 4D scene and its corresponding monaural audio. 2) Subsequently, to transform the monaural audio into spatial audio, we localize and track the sound sources within the 4D scene, where their 3D spatial coordinates at different timestamps are estimated via a pixel-level visual grounding strategy. 3) Based on the estimated sound source locations, we further synthesize plausible spatial audio that varies across different viewpoints and timestamps using physics-based simulation. Extensive experiments have demonstrated that our proposed method generates realistic spatial audio consistent with the synthesized 4D scene in a training-free manner, significantly enhancing the immersive experience for users. Generated audio and video examples are available at <https://x-drunker.github.io/Sonic4D-project-page>.

1 Introduction

Benefiting from large-scale data available [1, 2, 3] and recent advancement in generative models [4, 5], 4D generation (*i.e.*, dynamic 3D scene generation) [6, 7, 8, 9] has emerged as a promising direction due to its powerful capability in modeling complex spatiotemporal dynamics of real-world scenes. By enabling spatiotemporally consistent renderings from arbitrary camera viewpoints, 4D generation facilitates various downstream applications such as AR/VR [10, 11], robotics [12, 13], and autonomous driving [14, 15].

However, while existing 4D generation methods [13, 16, 17, 18] achieve impressive visual results, they typically neglect the generation of spatial audio consistent with the corresponding 4D scene (*i.e.*, audio that varies with the listener’s viewpoint and follows physical acoustic principles), limiting the overall immersive experience to a large extent.

To address this limitation, in this paper we propose Sonic4D, a novel framework that enables free-viewpoint rendering of both dynamic visual content and spatially consistent audio, thereby ensuring more immersive audiovisual exploration within the generated 4D scene. To this end, as shown in

*Equal Contribution

†Corresponding Authors

Fig. 1, we design a three-stage pipeline: **1) Dynamic Scene and Monaural Audio Generation.** To empower novel-view visual renderings and provide essential spatial priors for spatial audio generation, we first leverage a pre-trained 4D generative model to synthesize the dynamic 3D scene from a monocular video. In parallel, a video-to-audio generative model is utilized to produce monaural audio that is semantically aligned with the generated 4D scene, serving as the raw acoustic input for subsequent spatial audio rendering. **2) 3D Sound-Source Localization and Tracking.** To enable accurate physical simulation of dynamic sound propagation, we further estimate the sound source’s trajectory in 3D space (*i.e.*, the 3D locations of the sound source at different timestamps). To achieve this goal, we first use a multimodal large language model (MLLM) to perform pixel-level visual grounding on the input video, identifying the 2D coordinates of the sound source in each frame. These 2D positions are then back-projected onto the dynamic point cloud reconstructed in the previous stage, yielding a sequence of 3D coordinates that represent the sound source’s trajectory. **3) Physics-Driven Spatial Audio Synthesis.** Given the estimated sound source location and the generated 4D environment, a physics-based simulation using acoustic room impulse responses (RIRs) is employed to simulate plausible spatial audio, enabling more immersive experiences in complex 4D scenes.

Notably, our method adopts a modular architecture that facilitates the integration of state-of-the-art pre-trained expert models, ensuring that the framework remains extensible and future-proof, with performance continually improving as more advanced expert models become available.

The main contributions of this paper can be summarized as follows:

- We propose Sonic4D, a novel framework that achieves spatial audio generation for immersive 4D scene exploration. To the best of our knowledge, this is **the first work** that introduces spatial audio into the context of 4D generation.
- We propose a three-stage framework to achieve spatial audio generation: **1) Dynamic Scene and Monaural Audio Generation** to extract semantically aligned visual and audio priors from a single video; **2) 3D Sound-Source Localization and Tracking** to recover sound source’s 3D trajectory for precise acoustic simulation; **3) Physics-Driven Spatial Audio Synthesis** to render dynamic, viewpoint-adaptive binaural audio via physics-based room impulse response simulation.
- Extensive experiments have demonstrated that our framework can effectively generate spatial audio consistent with 4D visual content, enabling much more immersive and coherent audiovisual experiences.

2 Related Works

2.1 4D Generation

Early advances in 4D generation have built upon techniques such as Score Distillation Sampling (SDS) [19], which leverages generative priors of pre-trained diffusion models to optimize dynamic scene representations. For example, MAV3D [20] proposed a multi-stage framework that sequentially optimizes static geometry using text-to-image diffusion, followed by motion synthesis using text-to-video models. This paradigm laid the groundwork for methods such as Dream-in-4D [21], which further integrated motion priors from pretrained video diffusion models into dynamic NeRF-based representations [22, 23]. To improve rendering efficiency and motion fidelity, several methods have evolved from volumetric models to more expressive and compact formulations, such as AYG [24] and Trans4D [18], which employ deformation networks to animate static Gaussians across time. Concurrently, models like Consistent4D [6] and 4Diffusion [17] focused on enhancing spatiotemporal consistency, utilizing multiview interpolation, temporal alignment modules, or synchronized training strategies. Works such as Diffusion4D [25], PLA4D [26], and 4Dynamic [27] further emphasized controllability and efficiency by leveraging pixel-aligned supervision, video-based guidance, or hybrid representations combining mesh and Gaussian structures. Single-image driven methods like DreamGaussian4D [7], Human4DiT [28], and Animate124 [29] extended monocular inputs into coherent 4D outputs using hierarchical architectures or diffusion-based motion refinement. Recent studies such as Free4D [16] and MVTokenFlow [30] further improve spatial-temporal coherence and visual quality without tuning large generative models.

Though achieving remarkable results, all these methods focus solely on visual content rendering, neglecting the generation of spatial audio that aligns with the dynamic scene. In contrast, in this

paper we propose a novel framework for spatial audio generation that enables more coherent and immersive exploration of 4D scenes from arbitrary viewpoints.

2.2 Spatial Audio Generation

Early spatial audio generation methods [31, 32, 33] predominantly took monaural inputs and “binauralized” them via neural networks conditioned on visual cues. In recent years, the advent of powerful generative architectures has spurred end-to-end models that accept text prompts [34], images [34, 35], spatial parameters [36, 37], silent videos [38], or full 360° panoramas [39] to jointly learn semantic and spatial audio features. For example, SpatialSonic [34] leverages spatial-aware encoders and azimuth state matrices within a latent diffusion framework to provide fine-grained multimodal spatial guidance for stereo audio generation. ViSAGe [38] fuses CLIP visual embeddings with autoregressive neural audio codec modeling to generate coherent FOA directly from silent video frames. Recently, OmniAudio [39] addressed the 360° spatial audio gap by using a dual-branch architecture to fuse panoramic and FoV streams, enabling high-fidelity FOA generation from full spherical video content.

Although these methods benefit from the inherent capacity of generative models to capture complex multimodal distributions and yield impressive qualitative gains, they face two critical challenges. First, the data scarcity and domain gaps characteristic of end-to-end learning frameworks still constrain their ability to faithfully simulate spatial audio, resulting in suboptimal spatial rendering fidelity. Second, even when utilizing 360° video inputs, the synthesized sound field remains tied to the camera’s fixed pose and cannot account for dynamic listener motion or free-viewpoint changes within the scene.

Some alternative approaches [40, 41, 42] tackle spatial audio by jointly reconstructing novel views and associated audio given ground-truth recordings at specific viewpoints; these methods, however, are restricted to static scenes and focus on view-specific audio re-rendering. In contrast, our work decouples semantic audio synthesis from spatial rendering and employs room impulse response (RIR) convolution to robustly simulate the spatial acoustics perceived by a moving listener in dynamic environments.

2.3 Sound Source Localization

Sound source localization aims to find the location of sound sources in an image or video frame. Initial studies [43, 44, 45, 46] addressed this problem by leveraging methods like cross-modal attention and contrastive learning to establish effective alignment between audio and visual modalities, mainly focusing on single sound source localization. Some works have taken this further to achieve multi-sound source localization [47, 48, 49], enabling the simultaneous localization of multiple sound sources from mixed audio and visual inputs. However, these approaches focus on exploring audio–visual alignments and cannot localize sound sources without ground-truth audio. Moreover, due to the complexity of three- and even four-dimensional scenarios, few works [50] has addressed sound source detection or localization in 3D space.

Recently, the rapid advancement of Multimodal Large Language Models [51, 52, 53] (MLLMs) has made it possible to perform audio-visual grounding with strong generalization capabilities. In this work, we leverage the powerful prior knowledge of pretrained MLLMs to directly perform pixel-level visual grounding on the video input for sound source localization, followed by back-projection into 3D space to achieve accurate 3D sound source positioning and further spatial audio simulation.

3 Methods

Given a monocular input video $V^s = \{I_i^s\}_{i=1}^n \in \mathbb{R}^{n \times 3 \times H \times W}$, our goal is to generate both novel-view videos and corresponding spatial audio given arbitrary target camera trajectory $T^r = \{T_i^r\}_{i=1}^n \in \mathbb{R}^{n \times 4 \times 4}$, where each matrix T_i^r denotes the homogeneous camera pose at time i . As shown in Fig. 1, the overall pipeline is divided into three stages: 1) Dynamic scene and monaural audio generation; 2) 3D sound-source localization and tracking; 3) Physics-driven spatial audio synthesis. Each stage is discussed in detail in the following subsections.

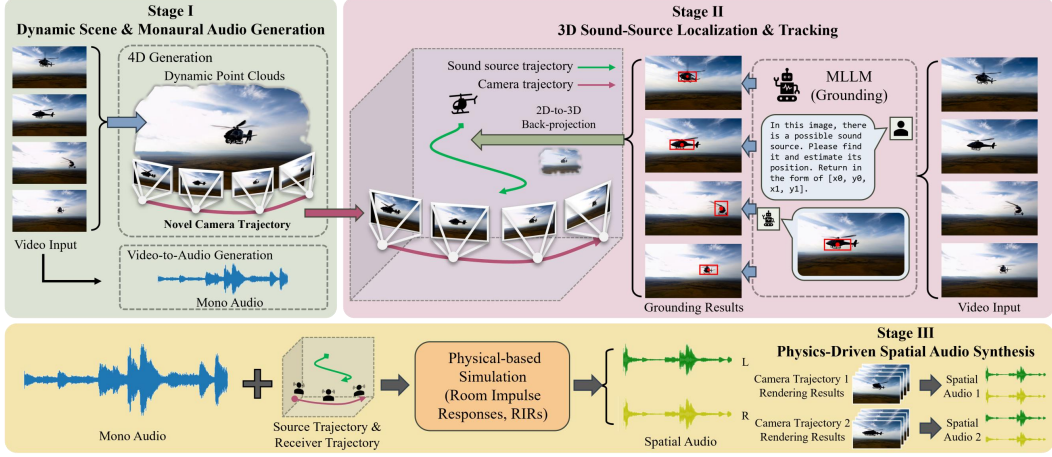


Figure 1: **Pipeline of Sonic4D.** Our method is composed of three stages: **1) Dynamic Scene and Monaural Audio Generation:** extracting semantically aligned visual scenes and audio priors from monocular videos (Sec. 3.1); **2) 3D Sound-Source Localization and Tracking:** estimating the sound source’s trajectory in 3D space for physically accurate sound propagation modeling (Sec. 3.2); **3) Physics-Driven Spatial Audio Synthesis:** leveraging a physics-based room impulse response simulation to realize spatial audio simulation. (Sec. 3.3)

3.1 Stage I: Dynamic Scene and Monaural Audio Generation

To obtain a novel-view video V^r while simultaneously capturing dynamic spatial priors for spatial audio simulation, a model that can produce high-fidelity, free-viewpoint renderings of dynamic scenes with strong spatiotemporal consistency is required. Motivated by recent progress in 4D generation, we adopt TrajectoryCrafter [54], a pretrained video generative model capable of synthesizing high-fidelity videos along arbitrary camera trajectories from a single-view input video, as our 4D content generator.

Specifically, we first apply a monocular depth estimator to estimate the depth maps $D^s = \{D_i^s\}_{i=1}^n \in \mathbb{R}^{n \times h \times w}$ of the input video V^s . Subsequently, we lift V^s into a set of dynamic point clouds $P = \{P_i\}_{i=1}^n$ using inverse perspective projection Φ^{-1} , which is formulated as follows:

$$P_i = \Phi^{-1}([I_i^s, D_i^s], K), \quad (1)$$

where $K \in \mathbb{R}^{3 \times 3}$ is the camera intrinsic matrix. Using the estimated dynamic point clouds, we synthesize novel-view renderings $I^r = \{I_i^r\}_{i=1}^n$ by projecting P onto the target camera trajectory $T^r = \{T_i^r\}_{i=1}^n \in \mathbb{R}^{n \times 4 \times 4}$ using the following equation:

$$I_i^r = \Phi(T_i^r \cdot P_i, K), \quad (2)$$

where Φ denotes the projection operation. The rendered results I^r are then used as conditioning inputs to the video diffusion model of TrajectoryCrafter, guiding the generation of high-fidelity novel-view videos.

Next, we prepare the raw monaural audio signal required for subsequent physics-based spatial audio simulation. To this end, we adopt MMAudio [55], a transformer-based video-to-audio synthesis model, to generate monaural audio $A^m \in \mathbb{R}^{1 \times T}$ that is temporally and semantically aligned with the input video V^s . By decomposing the task of immersive 4D scene exploration into two sub-tasks—*i.e.*, 4D scene generation and spatial audio synthesis—and leveraging pretrained expert models to extract the required visual and acoustic information, we can achieve greater flexibility and continually improve performance as upstream models evolve.

3.2 Stage II: 3D Sound Source Localization and Tracking

With the dynamic point cloud P and its associated monaural audio A^m , we proceed to localize and track the sound source in 3D space to facilitate physics-based spatial audio generation. However, directly tracking the sound source in a 4D environment remains highly challenging, particularly in

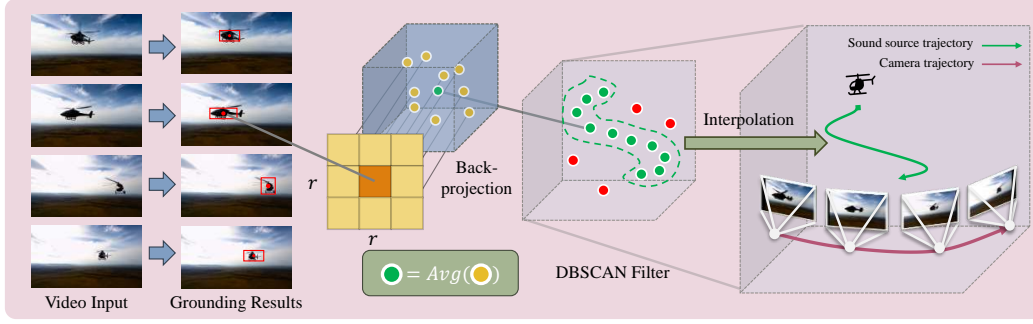


Figure 2: **Illustration of Stage II: 3D Sound Source Localization and Tracking.** We feed the video input frame-wisely into GroundingGPT [53] to obtain the sound source pixel coordinates. Then, we compute the average 3D coordinates of an $r \times r$ patch centered around the estimated 2D location via back-projection, and treat this as the 3D position of the sound source. Finally, we apply the DBSCAN [56] algorithm to filter and interpolate the sound-source trajectory, yielding a smooth and reliable final trajectory.

highly dynamic scenes with complex geometry. To address this, we first localize the sound source in the 2D pixel space and then back-project the estimated 2D coordinates into 3D space, thereby modeling the sound source trajectory within the generated dynamic scene.

To achieve this goal, existing 2D sound-source localization methods [46, 45, 57] typically require ground-truth audio inputs and are often tailored to specific scenarios and input sizes. This dependence on “true” audio runs counter to Sonic4D’s very generation-centric design. In contrast, given the rich commonsense knowledge and reasoning abilities of multimodal large language models (MLLMs), we propose to leverage GroundingGPT [53], a highly generalizable MLLM focused on grounding tasks and trained on a variety of audio–visual datasets for sound source localization, as our 2D sound source localization component.

Concretely, as shown in Fig. 1, we craft a textual prompt:

In this image, there is a possible sound source. Please find it and estimate its position. The only value you need to return is the position of the sound source in the format [x0, y0, x1, y1]. Do not include any text other than that.

and feed, frame by frame, the source video V^s together with the prompt into GroundingGPT [53]. Assuming the grounding result for the i -th frame I_i^s is represented by a bounding box $[x_0, y_0, x_1, y_1]$, we define the sound source pixel coordinates as the center of this bounding box, i.e.:

$$(u_i, v_i) = \left(\left\lfloor \frac{x_0 + x_1}{2} \times W \right\rfloor, \left\lfloor \frac{y_0 + y_1}{2} \times H \right\rfloor \right). \quad (3)$$

where W and H are the width and height of V^s . Let $d_i = D(u_i, v_i)$ denote the depth at pixel (u_i, v_i) . Then the 3D point of the sound source in camera coordinate system corresponding to frame i is given by

$$\mathbf{X}_i = \pi^{-1}((u_i, v_i), d_i). \quad (4)$$

Here, π^{-1} denotes the back-projection operator that maps a pixel coordinate and its depth into a 3D point. Considering the sporadic errors introduced by monocular depth estimation at individual pixels, we compute the 3D coordinates of an $r \times r$ pixel patch surrounding (u_i, v_i) and average them to obtain the sound-source’s 3D location as shown in Figure 2:

$$\bar{\mathbf{X}}_i = \frac{1}{|\mathcal{P}^r(u_i, v_i)|} \sum_{(u,v) \in \mathcal{P}^r(u_i, v_i)} \pi^{-1}((u, v), D(u, v)). \quad (5)$$

where $\mathcal{P}^r(u_i, v_i)$ denotes the set of all pixels (u, v) such that $|u - u_i| \leq (r - 1)/2$ and $|v - v_i| \leq (r - 1)/2$. Nonetheless, due to uncertainty in the bounding-box predictions, the back-projected trajectory $\{\bar{\mathbf{X}}_i\}$ may still exhibit significant fluctuations. To mitigate this, we apply DBSCAN [56] (Density-Based Spatial Clustering of Applications with Noise), a clustering-based outlier detection

algorithm that groups dense regions while marking sparse points as noise, to filter out spurious estimates. Points marked as noise are then temporally filled in via linear interpolation between the nearest non-noise neighbours to produce a smooth trajectory $\mathbf{Traj}_{src} = \{\mathbf{X}_i\}_{i=1}^n$.

In addition to the sound source’s trajectory, the receiver trajectory is also required for acoustic simulation. We use the user-specified camera trajectory as the receiver trajectory. For each frame i , the camera pose is defined as

$$\mathbf{T}_i^r = \begin{bmatrix} \mathbf{R}_i^r & \mathbf{t}_i^r \\ \mathbf{0}^\top & 1 \end{bmatrix}, \quad (6)$$

where $\mathbf{R}_i^r \in \mathbb{R}^{3 \times 3}$ is the rotation matrix and $\mathbf{t}_i^r \in \mathbb{R}^3$ is the translation vector. The receiver’s 3D position is therefore $\mathbf{r}_i = \mathbf{t}_i^r$, and the full receiver trajectory is $\mathbf{Traj}_{rsv} = \{\mathbf{r}_i\}_{i=1}^n$.

3.3 Stage III: Physics-Driven Spatial Audio Synthesis

Given the sound source’s trajectory \mathbf{Traj}_{src} , the receiver trajectory \mathbf{Traj}_{rsv} , and the monaural audio signal \mathbf{A}^m , we perform a physics-based spatial audio simulation.

A central element of our simulation is the computation of Room Impulse Responses (RIRs) via the Image Source Method (ISM) [58]. Building on the Image-Source Method for static RIRs, we apply gpuRIR [59] to simulate dynamic sources and receivers by segmenting the trajectories into short intervals over which they are assumed stationary. Concretely, let the total signal length be N samples and split it into M segments at sample indices

$$0 = n_0 < n_1 < \dots < n_M = N,$$

For each segment $i \in [1, M]$, let $\mathbf{x}_i^s = \mathbf{Traj}_{src}[i]$ denote the position of the sound source and $\mathbf{x}_i^r = \mathbf{Traj}_{rsv}[i]$ denote the position of the receiver. We simulate binaural microphone placement by offsetting from \mathbf{x}_i^r in the direction parallel to the camera’s rendering plane, yielding the left and right microphone positions $\mathbf{x}_{i,L}^r$ and $\mathbf{x}_{i,R}^r$. We compute the room impulse responses at the left and right microphones using the Image Source Method (ISM):

$$h_{i,L}(\tau) = \text{ISM}(\mathbf{x}_i^s, \mathbf{x}_{i,L}^r), \quad h_{i,R}(\tau) = \text{ISM}(\mathbf{x}_i^s, \mathbf{x}_{i,R}^r). \quad (7)$$

Let the mono audio block for segment i be

$$b_i[k] = \mathbf{A}^m[n_i + k], \quad 0 \leq k < n_{i+1} - n_i. \quad (8)$$

Then the left and right binaural signals are obtained by block-wise convolution:

$$y_L[n] = \sum_{i=0}^{M-1} (b_i * h_{i,L})[n - n_i], \quad y_R[n] = \sum_{i=0}^{M-1} (b_i * h_{i,R})[n - n_i], \quad (9)$$

where $h_{i,L}$ and $h_{i,R}$ are the left- and right-ear impulse responses in h_i . Putting it all together, the final binaural signal is

$$\mathbf{A}^b = (y_L[n], y_R[n]). \quad (10)$$

To ensure the output audio is in a valid range for playback, we normalize the signal to the range $[-1, 1]$:

$$\mathbf{A}^b \leftarrow \frac{\mathbf{A}^b}{\max(|\mathbf{A}^b|)}. \quad (11)$$

Compared with learning-based methods for spatial audio generation, our physics-based audio rendering ensures physical plausibility by explicitly modeling sound propagation using room impulse responses, resulting in more realistic spatial cues such as directionality and reverberation.

By decomposing the task into three modular stages, our framework maximizes flexibility and extensibility. Each stage benefits from pretraining or physical priors, allowing Sonic4D to scale with future advances in generative modeling and spatial simulation. Moreover, this decoupled design enables plug-and-play improvements, making Sonic4D suitable for a broad range of content creation and immersive applications.

4 Experiments

4.1 Experimental Settings

Since this is the first attempt to perform spatial audio generation for immersive 4D scene exploration, existing evaluation benchmarks are not directly applicable. Therefore, we conducted a user preference study to assess the perceptual quality of spatial audio generated by our proposed and other methods. We choose MMAudio [55] as the baseline method, whose generated audio is monaural and contains no spatialization.

To determine whether our generated spatial audio conveys a sense of space, we paired the same viewpoint-specific video with either the spatialized stereo audio or the non-spatialized mono audio for comparison. Participants were first asked, for each video pair (identical visuals but different audio), to choose which audio track felt more spatial. Next, they rated both audio tracks on two criteria from 1 to 5:

- **Spatial Localization Accuracy:** Measures how faithfully the interaural level and time-difference cues recreate the true 3D source position. Participants rate from 1 (“no sense of source direction”) to 5 (“precise and stable perception of source location”).
- **Audio-Visual Spatial Congruence:** Assesses how consistently the evolving audio cues (e.g. changes in loudness or binaural disparity) track the on-screen motion of the subject or camera. Participants rate from 1 (“audio movement conflicts with visuals”) to 5 (“audio shifts perfectly match visual motion”).

We recruited 25 participants, each of whom evaluated 33 video-audio pairs. All participants completed the experiment in a quiet environment while wearing binaural headphones. To more comprehensively demonstrate our model’s capabilities, we categorized the videos based on custom camera trajectories into **static** and **dynamic** viewpoints. Static viewpoints indicate using the original camera view unchanged or only modest transformations of that original view, with the viewpoint remaining fixed throughout; Dynamic viewpoints include translational camera movements, arc-shaped camera trajectories, and push-in/pull-back motions.

For data processing, we first excluded participants whose ratings exhibited low Pearson correlation with the overall preference distribution. We then computed and reported the preference percentages and mean opinion scores (MOS) across all viewpoints, as well as separately for static and dynamic viewpoints.

4.2 Quantitative Comparisons

Metric	All	Static viewpoints	Dynamic viewpoints
<i>Preference (%)</i>			
MMAudio [55]	10.97%	12.41%	9.90%
Sonic4D (<i>ours</i>)	89.03%	87.59%	90.10%
<i>MOS-SLA</i>			
MMAudio [55]	2.322	2.357	2.296
Sonic4D (<i>ours</i>)	4.013	3.986	4.033
<i>MOS-AVSC</i>			
MMAudio [55]	2.418	2.493	2.363
Sonic4D (<i>ours</i>)	3.977	3.980	3.975

Table 1: Subjective evaluation results for Sonic4D vs. MMAudio [55].

We present the results of user study evaluation comparing the spatial audio rendered by our method (Sonic4D) against the non-spatialized mono audio from MMAudio [55]. As shown in Table 1, Sonic4D achieved a strong overall preference rate of **89.03%**, indicating that the spatial audio generated by Sonic4D exhibits a significant perceptual difference in spatiality compared to the original mono audio, thus demonstrating the effectiveness of our model. This trend held consistently across

both static viewpoints (**87.59%**) and dynamic viewpoints (**90.10%**), demonstrating the robustness of our approach under varying camera trajectories.

In terms of Mean Opinion Scores (MOS), our method significantly outperforms the baseline in both evaluation dimensions. For **Spatial Localization Accuracy (MOS-SLA)**, Sonic4D achieved a mean score of **4.013**, compared to MMAudio [55]’s **2.322**. This suggests that participants were clearly able to perceive accurate and stable sound source positions when listening to our spatialized audio. A similar advantage is observed for **Audio–Visual Spatial Congruence (MOS-AVSC)**, where Sonic4D scored **3.977** versus **2.418** for MMAudio [55], indicating a much stronger alignment between auditory motion cues and on-screen visual dynamics.

Overall, these results validate that Sonic4D produces compelling and perceptually convincing spatial audio that generalizes well across diverse viewing conditions. Participants not only preferred the spatialized version, but also rated it higher in terms of spatial realism and audio-visual coherence, supporting the effectiveness of our approach in rendering viewpoint-consistent spatial audio.

4.3 Qualitative Comparisons

As shown in Fig. 3, we present additional qualitative comparisons with the baseline method. We predefined three types of camera trajectories: static viewpoint (case 1), camera circling around the subject (case 2), rightward panning and pulling out (case 3). For each case, we show the rendered video from the novel viewpoint, annotated with the motion direction of the visual subject within the frame. We then present the original waveform along with the stereo spatial audio waveform generated by Sonic4D. We highly recommend using headphones to listen to the specific examples provided in our supplementary material.

In case 1, the helicopter first moves leftward and then rightward across the frame, resulting in a perceived spatial effect where the sound shifts from being centered, to the left, and then to the right. By comparing **Regions 1 and 2** with **Regions 3 and 4** in the spatial audio waveform, we observe that the left channel initially has greater amplitude than the right. As the helicopter moves rightward, the left channel amplitude rapidly decreases and eventually falls below the right, aligning well with the expected spatial perception of the moving object. In case 2, the camera starts on the right side of a ukulele player and orbits to the left. The left-right disparity in **Regions 1 and 2**, as well as the temporal progression within those regions, closely mirrors the trajectory, indicating strong spatial tracking in the generated audio. Case 3 demonstrates that the same source video can yield notably different spatial audio depending on the camera motion, validating the view-dependence of our model. In video 1, as the camera pans rightward, the fountain becomes closer to the left ear, leading to increased amplitude in the left channel (**Regions 1,2**). In video 2, the camera gradually pulls out, producing a fading splash sound that matches the increasing distance (**Regions 3,4,5,6**).

These qualitative results demonstrate that the spatial audio generated by Sonic4D aligns closely with the visual cues, reflecting both spatial position and dynamic changes in the scene.

5 Conclusions

In this paper, we present Sonic4D, a novel paradigm that enables spatial audio generation for immersive 4D scene exploration. Specifically, our method consists of three stages: **1) Dynamic Scene and Monaural Audio Generation:** we first employ pre-trained expert models to generate the 4D scene and its corresponding monaural audio, aiming to provide sufficient spatial and acoustic priors for subsequent spatial audio simulation. **2) 3D Sound-Source Localization and Tracking:** we further propose a pixel-level visual grounding strategy to estimate the sound source’s trajectory in 3D space, facilitating spatial alignment between audio and visual content in dynamic scenes. **3) Physics-Driven Spatial Audio Synthesis:** Based on the estimated sound source’s trajectory, we synthesize plausible, viewpoint-adaptive spatial audio using physics-based room impulse response (RIR) simulation. Extensive experiments demonstrate that our proposed method generates realistic spatial audio that is consistent with the synthesized 4D scene in a training-free manner, significantly enhancing the user’s immersive experience.

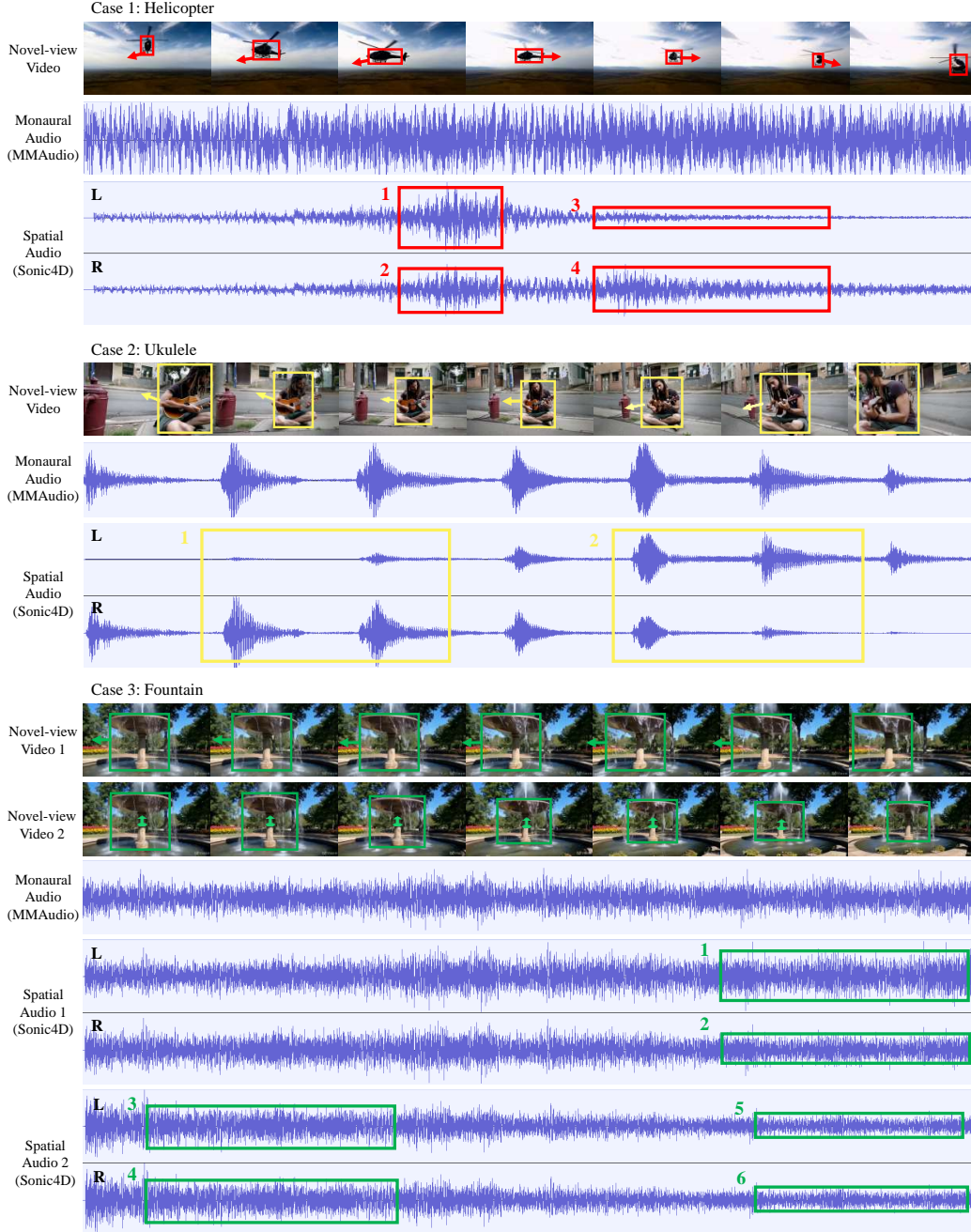


Figure 3: **Qualitative results across different scenarios.** We present comparisons of the spatial audio generated by Sonic4D conditioning on various camera trajectories, including static camera viewpoints, camera circling around the subject, rightward panning, and pulling out. These examples demonstrate the temporal and spatial alignment between the generated spatial audio and the motion of the visual subject.

6 Limitations

Although our method can generate spatial audio that follows the camera viewpoint with clear directional cues, it still has several potential limitations:

- While we model the dynamic trajectories of both the sound source and the listener using physics-based methods, the quality of the synthesized binaural audio may still be limited due to the lack of fine-grained acoustic simulation, such as incorporating Head-Related Transfer Functions (HRTF) or complex wave-based propagation models.
- For simplicity, we constrain our setup to a single sound source per video. However, thanks to the flexibility of our framework, multi-source localization and generation can be supported by modifying the prompts provided to GroundingGPT and MMAudio accordingly.
- Our use of monocular depth-derived point clouds lacks detailed geometric modeling, which may limit the physical accuracy of spatial audio propagation in complex environments.

References

- [1] Khurram Soomro, Amir Roshan Zamir, and Mubarak Shah. Ucf101: A dataset of 101 human actions classes from videos in the wild. *arXiv preprint arXiv:1212.0402*, 2012.
- [2] Christoph Schuhmann, Richard Vencu, Romain Beaumont, Robert Kaczmarczyk, Clayton Mullis, Aarush Katta, Theo Coombes, Jenia Jitsev, and Aran Komatsuzaki. Laion-400m: Open dataset of clip-filtered 400 million image-text pairs. *arXiv preprint arXiv:2111.02114*, 2021.
- [3] Jianhui Yu, Hao Zhu, Liming Jiang, Chen Change Loy, Weidong Cai, and Wayne Wu. Celebv-text: A large-scale facial text-video dataset. In *Proceedings of the IEEE/CVF Conference on Computer Vision and Pattern Recognition*, pages 14805–14814, 2023.
- [4] Jonathan Ho, Ajay Jain, and Pieter Abbeel. Denoising diffusion probabilistic models. *Advances in neural information processing systems*, 33:6840–6851, 2020.
- [5] Jiaming Song, Chenlin Meng, and Stefano Ermon. Denoising diffusion implicit models. *arXiv preprint arXiv:2010.02502*, 2020.
- [6] Yanqin Jiang, Li Zhang, Jin Gao, Weiming Hu, and Yao Yao. Consistent4d: Consistent 360° dynamic object generation from monocular video. In *The Twelfth International Conference on Learning Representations*, 2024.
- [7] Jiawei Ren, Liang Pan, Jiaxiang Tang, Chi Zhang, Ang Cao, Gang Zeng, and Ziwei Liu. Dreamgaussian4d: Generative 4d gaussian splatting. *arXiv preprint arXiv:2312.17142*, 2023.
- [8] Yifei Zeng, Yanqin Jiang, Siyu Zhu, Yuanxun Lu, Youtian Lin, Hao Zhu, Weiming Hu, Xun Cao, and Yao Yao. Stag4d: Spatial-temporal anchored generative 4d gaussians. In *European Conference on Computer Vision*, pages 163–179. Springer, 2024.
- [9] Hanxin Zhu, Tianyu He, Xiqian Yu, Junliang Guo, Zhibo Chen, and Jiang Bian. Ar4d: Autoregressive 4d generation from monocular videos. *arXiv preprint arXiv:2501.01722*, 2025.
- [10] Renjie Li, Panwang Pan, Bangbang Yang, Dejie Xu, Shijie Zhou, Xuanyang Zhang, Zeming Li, Achuta Kadambi, Zhangyang Wang, Zhengzhong Tu, et al. 4k4dgen: Panoramic 4d generation at 4k resolution. *arXiv preprint arXiv:2406.13527*, 2024.
- [11] Dieter Fritsch and Michael Klein. 3d and 4d modeling for ar and vr app developments. In *2017 23rd International Conference on Virtual System & Multimedia (VSMM)*, pages 1–8. IEEE, 2017.
- [12] Muhammad Yasir Khalid, Zia Ullah Arif, Waqas Ahmed, Rehan Umer, Ali Zolfagharian, and Mahdi Bodaghi. 4d printing: Technological developments in robotics applications. *Sensors and Actuators A: Physical*, 343:113670, 2022.
- [13] Sung Yun Hann, Haitao Cui, Margaret Nowicki, and Lijie Grace Zhang. 4d printing soft robotics for biomedical applications. *Additive Manufacturing*, 36:101567, 2020.
- [14] Lening Wang, Wenzhao Zheng, Yilong Ren, Han Jiang, Zhiyong Cui, Haiyang Yu, and Jiwen Lu. Occsora: 4d occupancy generation models as world simulators for autonomous driving. *arXiv preprint arXiv:2405.20337*, 2024.

- [15] Chen Min, Dawei Zhao, Liang Xiao, Jian Zhao, Xinli Xu, Zheng Zhu, Lei Jin, Jianshu Li, Yulan Guo, Junliang Xing, et al. Driveworld: 4d pre-trained scene understanding via world models for autonomous driving. In *Proceedings of the IEEE/CVF Conference on Computer Vision and Pattern Recognition*, pages 15522–15533, 2024.
- [16] Tianqi Liu, Zihao Huang, Zhaoxi Chen, Guangcong Wang, Shoukang Hu, liao Shen, Huiqiang Sun, Zhiguo Cao, Wei Li, and Ziwei Liu. Free4d: Tuning-free 4d scene generation with spatial-temporal consistency. *arXiv preprint arXiv:2503.20785*, 2025.
- [17] Haiyu Zhang, Xinyuan Chen, Yaohui Wang, Xihui Liu, Yunhong Wang, and Yu Qiao. 4diffusion: Multi-view video diffusion model for 4d generation. *arXiv preprint arXiv:2405.20674*, 2024.
- [18] Bohan Zeng, Ling Yang, Siyu Li, Jiaming Liu, Zixiang Zhang, Juanxi Tian, Kaixin Zhu, Yongzhen Guo, Fu-Yun Wang, Minkai Xu, Stefano Ermon, and Wentao Zhang. Trans4d: Realistic geometry-aware transition for compositional text-to-4d synthesis. *arXiv preprint arXiv:2410.07155*, 2024.
- [19] Ben Poole, Ajay Jain, Jonathan T. Barron, Ben Mildenhall, Pieter Abbeel, and Pratul Srinivasan. Dreamfusion: Text-to-3d using 2d diffusion. In *Advances in Neural Information Processing Systems (NeurIPS)*, 2022.
- [20] Uriel Singer, Shelly Sheynin, Adam Polyak, Oron Ashual, Iurii Makarov, Filippos Kokkinos, Naman Goyal, Andrea Vedaldi, Devi Parikh, Justin Johnson, and Yaniv Taigman. Text-to-4d dynamic scene generation. *arXiv:2301.11280*, 2023.
- [21] Yufeng Zheng, Xueting Li, Koki Nagano, Sifei Liu, Otmar Hilliges, and Shalini De Mello. A unified approach for text- and image-guided 4d scene generation. In *CVPR*, 2024.
- [22] Albert Pumarola, Enric Corona, Gerard Pons-Moll, and Francesc Moreno-Noguer. D-nerf: Neural radiance fields for dynamic scenes. In *Proceedings of the IEEE/CVF conference on computer vision and pattern recognition*, pages 10318–10327, 2021.
- [23] Zhiwen Yan, Chen Li, and Gim Hee Lee. Nerf-ds: Neural radiance fields for dynamic specular objects. In *Proceedings of the IEEE/CVF Conference on Computer Vision and Pattern Recognition*, pages 8285–8295, 2023.
- [24] Huan Ling, Seung Wook Kim, Antonio Torralba, Sanja Fidler, and Karsten Kreis. Align your gaussians: Text-to-4d with dynamic 3d gaussians and composed diffusion models. In *IEEE Conference on Computer Vision and Pattern Recognition (CVPR)*, 2024.
- [25] Hanwen Liang, Yuyang Yin, Dejia Xu, Hanxue Liang, Zhangyang Wang, Konstantinos N Plataniotis, Yao Zhao, and Yunchao Wei. Diffusion4d: Fast spatial-temporal consistent 4d generation via video diffusion models. *arXiv preprint arXiv:2405.16645*, 2024.
- [26] Qiaowei Miao, Jinsheng Quan, Kehan Li, and Yawei Luo. Pla4d: Pixel-level alignments for text-to-4d gaussian splatting. *arXiv preprint arXiv:2405.19957*, 2024.
- [27] Yu-Jie Yuan, Leif Kobbelt, Jiwen Liu, Yuan Zhang, Pengfei Wan, Yu-Kun Lai, and Lin Gao. 4dynamic: Text-to-4d generation with hybrid priors. *arXiv preprint arXiv:2407.12684*, 2024.
- [28] Ruizhi Shao, Youxin Pang, Zerong Zheng, Jingxiang Sun, and Yebin Liu. Human4dit: 360-degree human video generation with 4d diffusion transformer. *ACM Transactions on Graphics (TOG)*, 43(6), 2024.
- [29] Yuyang Zhao, Zhiwen Yan, Enze Xie, Lanqing Hong, Zhenguo Li, and Gim Hee Lee. Animate124: Animating one image to 4d dynamic scene. *arXiv preprint arXiv:2311.14603*, 2023.
- [30] Hanzhuo Huang, Yuan Liu, Ge Zheng, Jiepeng Wang, Zhiyang Dou, and Sibe Yang. Mvtoken-flow: High-quality 4d content generation using multiview token flow. In *Proceedings of the International Conference on Learning Representations (ICLR)*, 2025.
- [31] Ruohan Gao and Kristen Grauman. 2.5 d visual sound. In *Proceedings of the IEEE/CVF Conference on Computer Vision and Pattern Recognition*, pages 324–333, 2019.

- [32] Xudong Xu, Hang Zhou, Ziwei Liu, Bo Dai, Xiaogang Wang, and Dahua Lin. Visually informed binaural audio generation without binaural audios. In *Proceedings of the IEEE/CVF Conference on Computer Vision and Pattern Recognition*, pages 15485–15494, 2021.
- [33] Yichong Leng, Zehua Chen, Junliang Guo, Haohe Liu, Jiawei Chen, Xu Tan, Danilo Mandic, Lei He, Xiangyang Li, Tao Qin, et al. Binauralgrad: A two-stage conditional diffusion probabilistic model for binaural audio synthesis. *Advances in Neural Information Processing Systems*, 35:23689–23700, 2022.
- [34] Peiwen Sun, Sitong Cheng, Xiangtai Li, Zhen Ye, Huadai Liu, Honggang Zhang, Wei Xue, and Yike Guo. Both ears wide open: Towards language-driven spatial audio generation. *arXiv preprint arXiv:2410.10676*, 2024.
- [35] Rishit Dagli, Shivesh Prakash, Robert Wu, and Houman Khosravani. See-2-sound: Zero-shot spatial environment-to-spatial sound. *arXiv preprint arXiv:2406.06612*, 2024.
- [36] Mojtaba Heydari, Mehrez Souden, Bruno Conejo, and Joshua Atkins. Immersediffusion: A generative spatial audio latent diffusion model. In *ICASSP 2025-2025 IEEE International Conference on Acoustics, Speech and Signal Processing (ICASSP)*, pages 1–5. IEEE, 2025.
- [37] Saksham Singh Kushwaha, Jianbo Ma, Mark RP Thomas, Yapeng Tian, and Avery Bruni. Diff-sage: End-to-end spatial audio generation using diffusion models. In *ICASSP 2025-2025 IEEE International Conference on Acoustics, Speech and Signal Processing (ICASSP)*, pages 1–5. IEEE, 2025.
- [38] Jaeyeon Kim, Heeseung Yun, and Gunhee Kim. Visage: Video-to-spatial audio generation. In *The Thirteenth International Conference on Learning Representations*, 2025.
- [39] Huadai Liu, Tianyi Luo, Qikai Jiang, Kaicheng Luo, Peiwen Sun, Jialei Wan, Rongjie Huang, Qian Chen, Wen Wang, Xiangtai Li, et al. Omniaudio: Generating spatial audio from 360-degree video. *arXiv preprint arXiv:2504.14906*, 2025.
- [40] Changan Chen, Alexander Richard, Roman Shapovalov, Vamsi Krishna Ithapu, Natalia Neverova, Kristen Grauman, and Andrea Vedaldi. Novel-view acoustic synthesis. In *Proceedings of the IEEE/CVF Conference on Computer Vision and Pattern Recognition*, pages 6409–6419, 2023.
- [41] Susan Liang, Chao Huang, Yapeng Tian, Anurag Kumar, and Chenliang Xu. Av-nerf: Learning neural fields for real-world audio-visual scene synthesis. *Advances in Neural Information Processing Systems*, 36:37472–37490, 2023.
- [42] Mingfei Chen and Eli Shlizerman. Av-cloud: Spatial audio rendering through audio-visual cloud splatting. *Advances in Neural Information Processing Systems*, 37:141021–141044, 2024.
- [43] Arda Senocak, Tae-Hyun Oh, Junsik Kim, Ming-Hsuan Yang, and In So Kweon. Learning to localize sound source in visual scenes. In *Proceedings of the IEEE conference on computer vision and pattern recognition*, pages 4358–4366, 2018.
- [44] Honglie Chen, Weidi Xie, Triantafyllos Afouras, Arsha Nagrani, Andrea Vedaldi, and Andrew Zisserman. Localizing visual sounds the hard way. In *Proceedings of the IEEE/CVF conference on computer vision and pattern recognition*, pages 16867–16876, 2021.
- [45] Arda Senocak, Hyeonggon Ryu, Junsik Kim, Tae-Hyun Oh, Hanspeter Pfister, and Joon Son Chung. Sound source localization is all about cross-modal alignment. In *Proceedings of the IEEE/CVF international conference on computer vision*, pages 7777–7787, 2023.
- [46] Sung Jin Um, Dongjin Kim, and Jung Uk Kim. Audio-visual spatial integration and recursive attention for robust sound source localization. In *Proceedings of the 31st ACM International Conference on Multimedia*, pages 3507–3516, 2023.
- [47] Di Hu, Rui Qian, Minyue Jiang, Xiao Tan, Shilei Wen, Errui Ding, Weiyao Lin, and Dejing Dou. Discriminative sounding objects localization via self-supervised audiovisual matching. *Advances in Neural Information Processing Systems*, 33:10077–10087, 2020.

- [48] Shentong Mo and Yapeng Tian. Audio-visual grouping network for sound localization from mixtures. In *Proceedings of the IEEE/CVF conference on computer vision and pattern recognition*, pages 10565–10574, 2023.
- [49] Dongjin Kim, Sung Jin Um, Sangmin Lee, and Jung Uk Kim. Learning to visually localize sound sources from mixtures without prior source knowledge. In *Proceedings of the IEEE/CVF Conference on Computer Vision and Pattern Recognition*, pages 26467–26476, 2024.
- [50] Yuhang He, Sangyun Shin, Anoop Cherian, Niki Trigoni, and Andrew Markham. Sound3dvdet: 3d sound source detection using multiview microphone array and rgb images. In *Proceedings of the IEEE/CVF Winter Conference on Applications of Computer Vision*, pages 5496–5507, 2024.
- [51] Yang Zhao, Zhijie Lin, Daquan Zhou, Zilong Huang, Jiashi Feng, and Bingyi Kang. Bubogpt: Enabling visual grounding in multi-modal llms. *arXiv preprint arXiv:2307.08581*, 2023.
- [52] Shehan Munasinghe, Hanan Gani, Wenqi Zhu, Jiale Cao, Eric Xing, Fahad Shahbaz Khan, and Salman Khan. Videoglamm: A large multimodal model for pixel-level visual grounding in videos. *arXiv preprint arXiv:2411.04923*, 2024.
- [53] Zhaowei Li, Qi Xu, Dong Zhang, Hang Song, Yiqing Cai, Qi Qi, Ran Zhou, Junting Pan, Zefeng Li, Van Tu Vu, et al. Groundinggpt: Language enhanced multi-modal grounding model. *arXiv preprint arXiv:2401.06071*, 2024.
- [54] Mark YU, Wenbo Hu, Jinbo Xing, and Ying Shan. Trajectorycrafter: Redirecting camera trajectory for monocular videos via diffusion models. *arXiv preprint arXiv:2503.05638*, 2025.
- [55] Ho Kei Cheng, Masato Ishii, Akio Hayakawa, Takashi Shibuya, Alexander Schwing, and Yuki Mitsufuji. Taming multimodal joint training for high-quality video-to-audio synthesis. *arXiv preprint arXiv:2412.15322*, 2024.
- [56] Martin Ester, Hans-Peter Kriegel, Jörg Sander, Xiaowei Xu, et al. A density-based algorithm for discovering clusters in large spatial databases with noise. In *kdd*, volume 96, pages 226–231, 1996.
- [57] Sooyoung Park, Arda Senocak, and Joon Son Chung. Can clip help sound source localization? In *Proceedings of the IEEE/CVF Winter Conference on Applications of Computer Vision*, pages 5711–5720, 2024.
- [58] Jont B Allen and David A Berkley. Image method for efficiently simulating small-room acoustics. *The Journal of the Acoustical Society of America*, 65(4):943–950, 1979.
- [59] David Diaz-Guerra, Antonio Miguel, and Jose R Beltran. gpurir: A python library for room impulse response simulation with gpu acceleration. *Multimedia Tools and Applications*, 80(4):5653–5671, 2021.
- [60] Kuaishou Technology. Kling ai text-to-video, 2024. <https://klingai.com/text-to-video>.
- [61] CapCut. Dreamina: Free ai image generator - create art & images from text, 2025. <https://dreamina.capcut.com/>.
- [62] Fan Bao, Chendong Xiang, Gang Yue, Guande He, Hongzhou Zhu, Kaiwen Zheng, Min Zhao, Shilong Liu, Yaole Wang, and Jun Zhu. Vidu: a highly consistent, dynamic and skilled text-to-video generator with diffusion models. *arXiv preprint arXiv:2405.04233*, 2024.

A Details of User Study

A.1 Experiment Setup and Procedure

The user study consists of three main stages:

Step 1: Dynamic Scene and Monaural Audio Generation. In the first stage of our pipeline, as described in the *Dynamic Scene and Monaural Audio Generation* section, we used TrajectoryCrafter [54] to predict dynamic point clouds for 4D scene construction. Since TrajectoryCrafter [54] uses the relative transformation between the user-specified camera trajectory and the source camera as the basis for novel view rendering and requires a stabilized source video, we selected only source videos that meet this requirement. To generate these videos, we manually composed prompts for commercial text-to-video models (e.g., Kling [60], Dreamina [61], Vidu [62]), and for each sample, we designed a custom camera trajectory to render the target view. We then leveraged Sonic4D to generate both the novel view video and the corresponding spatialized audio.

Step 2: Interface Setup and Counterbalancing. As illustrated in Figure 4, we created a local web-based interface to facilitate user evaluation. The landing page provided clear instructions on the task and rating criteria as shown in 4a. We created 33 question pages for participants to complete. To ensure counterbalancing, we randomized the order of all audio-video pairs as shown in 4b, as well as the internal ordering of each pair (left/right assignment), to mitigate any potential order effects or positional biases. Participants were asked to rate each video on the following two aspects using a 5-point Likert scale. The detailed rating criteria are as follows:

- **Spatial Localization Accuracy:**
 - 5 – The position of the subject or camera can be clearly perceived from the audio.
 - 4 – The direction or positional changes can generally be perceived.
 - 3 – Some spatial positioning is conveyed through the audio.
 - 2 – Audio provides vague or weak spatial cues.
 - 1 – Little to no sense of spatial position from the audio.
- **Audio–Visual Spatial Congruence:**
 - 5 – The direction indicated by audio cues (e.g., volume changes, binaural differences) perfectly matches the visual motion.
 - 4 – The audio directionality mostly matches the visuals.
 - 3 – The audio and visual alignment is partially consistent.
 - 2 – The audio and visuals are misaligned or direction is hard to perceive.
 - 1 – The spatial audio cues conflict with or fail to reflect the visuals.

Step 3: Data Collection and Filtering. After collecting all participant responses regarding spatial audio preference and ratings, we computed the Pearson correlation between each participant’s responses and the overall average responses. Specifically, for each participant i , we encode their answers on all preference questions as a numerical vector $\mathbf{a}^{(i)}$, where each answer is mapped to a scalar:

$$a_j^{(i)} = \begin{cases} 1, & \text{if the participant preferred Video 1} \\ 2, & \text{if the participant preferred Video 2} \\ 0, & \text{if the participant selected “Almost same”} \end{cases} \quad (12)$$

Here, $a_j^{(i)}$ denotes the response of the i -th participant to the j -th question, where $j = 1, 2, \dots, M$. The full response vector for participant i is:

$$\mathbf{a}^{(i)} = [a_1^{(i)}, a_2^{(i)}, \dots, a_M^{(i)}]$$

We then compute the mean preference vector across all N participants:

$$\bar{\mathbf{a}} = \frac{1}{N} \sum_{i=1}^N \mathbf{a}^{(i)} \quad (13)$$

Sonic4D Subjective Evaluation Instructions

Before You Begin:

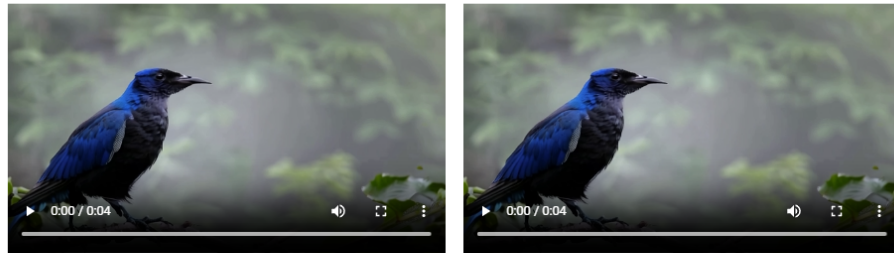
- Please use a PC browser such as Chrome or Edge to complete the study.
- Make sure you are in a quiet environment during the experiment.
- **Wear binaural headphones** throughout the study. On Windows 11, we recommend setting your volume to 40 or higher.

Procedure:

- The study consists of 33 video pairs and takes approximately 20 minutes.
- On each question page, you will watch two videos with identical visuals but different audio. Please listen carefully to the sound.
- After watching the videos, you will answer the following three questions:
 1. **Which video has better spatial perception in terms of overall audio experience?**
 2. **Please rate the spatial localization accuracy of each video on a scale from 1 to 5 (1 = worst, 5 = best):**
 - 5 - The position of the subject or camera can be clearly perceived from the audio
 - 4 - The direction or changes in the position can generally be perceived
 - 3 - Some spatial positioning is conveyed through the audio
 - 2 - Audio provides vague or weak spatial cues
 - 1 - Little to no sense of spatial position from the audio
 3. **Please rate the audio-visual spatial congruence of each video on a scale from 1 to 5 (1 = worst, 5 = best):**
 - 5 - The direction indicated by audio cues (e.g., volume changes, binaural differences) perfectly matches the visual motion
 - 4 - The audio directionality mostly matches the visuals
 - 3 - The audio and visual alignment is partially consistent
 - 2 - The audio and visuals are misaligned or direction is hard to perceive
 - 1 - The spatial audio cues conflict with or fail to reflect the visuals
- After completing all questions, please return the saved JSON file containing your responses.

Start Experiment

(a) User study instruction page outlining participation guidelines and evaluation criteria.



Which video has better spatial perception in terms of overall audio performance?

Please rate the audio positional awareness of the videos respectively. (1 being the worst, 5 being the best).

Video 1

Video 2

Please rate the audio-visual spatial alignment of the videos respectively. (1 being the worst, 5 being the best)

Video 1

Video 2

Previous

Next

(b) Example of a user study question page, displaying paired videos and corresponding rating options.

Figure 4: Screenshots of the user study interface.

Next, the Pearson correlation coefficient between each participant’s response vector and the mean vector is computed as:

$$r^{(i)} = \frac{\sum_{j=1}^M (a_j^{(i)} - \bar{a}^{(i)}) (\bar{a}_j - \bar{a})}{\sqrt{\sum_{j=1}^M (a_j^{(i)} - \bar{a}^{(i)})^2} \sqrt{\sum_{j=1}^M (\bar{a}_j - \bar{a})^2}} \quad (14)$$

where M is the number of preference questions, $\bar{a}^{(i)}$ is the mean of participant i ’s answers, and \bar{a} is the mean of the overall mean vector $\bar{\mathbf{a}}$.

We exclude participant i if $r^{(i)} < 0.4$, considering such responses to be poorly correlated with the overall trend. In the end, we retained 22 valid participant responses, and calculated the final Mean Opinion Scores (MOS) based on these.

A.2 Experimental Video Categories

To analyze the impact of different viewpoint conditions on spatial audio perception, we categorized the evaluation videos into two major groups: *static* and *dynamic* viewpoints.

A video is considered to have a **static viewpoint** if the camera position is fixed throughout the clip, or undergoes only minor transformations of original camera pose but still remains fixed. In contrast, a **dynamic viewpoint** involves explicit camera motion, such as linear translation, arc-shaped trajectories around a subject, or push-in/pull-back zooming effects that create continuous changes in perspective.

To ensure a balanced evaluation, we selected a diverse set of examples from each category, as summarized in Table 2. The dataset includes a roughly balanced distribution of static and dynamic scenarios.

View Type	Subtype	Number of Samples
Static	Raw viewpoint (static sound source)	3
	Raw viewpoint (dynamic sound source)	7
	Fixed camera (transformation)	4
Total (Static)		14
Dynamic	Translational movement	5
	Arc-shaped trajectory	7
	Push-in / Pull-back	7
Total (Dynamic)		19

Table 2: Distribution of evaluation videos by viewpoint category

B Details of Physics-Driven Spatial Audio Synthesis

Room Impulse Response (RIR) plays a crucial role in spatial audio rendering by modeling how sound propagates and reflects within an environment. Accurate RIR simulation enables the synthesis of physically plausible spatial cues, enhancing the realism of the generated audio experience.

In our pipeline, we adopt gpuRIR [59] as the simulator to generate synthetic RIRs. To reflect varying acoustic environments, we predefine four types of room size categories with randomly sampled dimensions in meters, as shown below:

- **Small:** Length and width $\in [3, 8]$, height $\in [2.5, 4]$
- **Medium:** Length and width $\in [8, 15]$, height $\in [3, 6]$
- **Large:** Length and width $\in [15, 30]$, height $\in [5, 10]$
- **Outdoor:** Length and width $\in [100, 200]$, height $\in [50, 100]$

For each category, the length, width, and height are randomly sampled within the corresponding range. Given the source and receiver trajectories derived in Stage 2, we compute the minimal bounding cuboid that encapsulates both trajectories. This cuboid is then placed at the center of the room. If the bounding box exceeds the selected room size, it is uniformly scaled down to fit the lower bounds of the selected category.

To ensure smooth transitions and minimize auditory artifacts, we perform temporal upsampling on the trajectories before simulation. Specifically, we use a high-resolution sampling rate of $n = 44100$ points per trajectory.

For microphone orientation, we support two polar patterns: omnidirectional (*omni*) and cardioid (*card*). In the cardioid setting, the microphone orientation at each point is aligned to face outward from the center plane of the rendering space.

Finally, the reverberation time (T_{60}) is randomly sampled from a uniform distribution in the range (0.3, 0.6) seconds to simulate varying acoustic characteristics across environments.